Small extracellular vesicles derived from mesenchymal stromal cells mitigate intestinal toxicity in a mouse model of acute radiation syndrome.

Alison Accarie
Institut de Radioprotection et de Surete Nucleaire
Bruno L'homme
Institut de Radioprotection et de Surete Nucleaire
Mohamedamine Benadjaoud
Institut de Radioprotection et de Surete Nucleaire
Sai Kiang Lim
National University of Singapore
Chadan Guha
Albert Einstein Medical Center
Marc Benderitter
Institut de Radioprotection et de Surete Nucleaire
Radia Tamarat
Institut de Radioprotection et de Surete Nucleaire
Alexandra SEMONT (semonta@yahoo.com)
Institut de Radioprotection et de Surete Nucleaire https://orcid.org/0000-0003-3444-5895

Research

Keywords: acute radiation syndrome, gastrointestinal syndrome, intestinal epithelial barrier, medical countermeasures, mesenchymal stromal cell-derived small extracellular vesicles, exosomes

Posted Date: March 5th, 2020

DOI: https://doi.org/10.21203/rs.3.rs-16132/v1

Version of Record: A version of this preprint was published on August 27th, 2020. See the published version at https://doi.org/10.1186/s13287-020-01887-1.

Abstract

Background: Human exposure to high doses of radiation resulting in acute radiation syndrome and death could rapidly escalate to a mass casualty catastrophe in the event of nuclear accidents or terrorism. The primary reason is that there is presently no effective treatment option, especially for radiation-induced gastrointestinal syndrome. This syndrome results from disruption of mucosal barrier integrity leading to severe dehydration, blood loss and sepsis. In this study, we tested whether small extracellular vesicles/exosomes derived from mesenchymal stromal cells (MSC) could reduce radiation-related mucosal barrier damage and reduce radiation-induced animal mortality.

Methods: Human MSC-derived small extracellular vesicles/exosomes were intravenously administered to NUDE mice, 3, 24 and 48 hours after lethal whole-body irradiation (10 Gy). Integrity of the small intestine epithelial barrier was assessed by morphologic analysis, immunostaining for tight junction protein (claudin-3) and *in vivo* permeability to 4 kDa FITC-labeled dextran. Renewal of small intestinal epithelium was determined by the quantification of epithelial cell apoptosis (TUNEL staining) and proliferation (Ki67 immunostaining). Statistical analyses were performed using one-way ANOVA followed by a Tukey test. Statistical analyses of mouse survival were performed using the methods of Kaplan-Meier and Cox.

Results: We demonstrated that MSC-derived small extracellular vesicles/exosomes treatment reduced by 85% the instantaneous mortality risk in mice subjected to 10 Gy whole-body irradiation and thus increased their survival time. This effect could be attributed to the efficacy of MSC-derived small extracellular vesicles/exosomes in reducing mucosal barrier disruption. We showed that MSC-derived small extracellular vesicles/exosomes improved renewal of the small intestinal epithelium by stimulating proliferation and inhibiting apoptosis of the epithelial crypt cells. MSC-derived small extracellular vesicles/exosomes also reduced radiation-induced mucosal permeability as evidenced by the preservation of claudin-3 immunostaining at the tight junctions of the epithelium.

Conclusions: MSC-derived small extracellular vesicles/exosomes promote epithelial repair and regeneration and preserve structural integrity of the intestinal epithelium in mice exposed to radiation-induced gastrointestinal toxicity. Our results suggest that the administration of MSC-derived small extracellular vesicles/exosomes could be a treatment modality to limit acute radiation syndrome.

Introduction

Accidental or intended catastrophic nuclear/radiological events represent a real threat of mass casualty catastrophe. In such events, exposed victims would be considered “at increased risk” of developing exposure-related morbidity and/or mortality, called acute radiation syndrome (ARS). Whole-body irradiation (WBI) doses can be divided into potentially sublethal (≤ 2 Gy), lethal (between 2 and 10 Gy) and supralethal (≥ 10 Gy). For doses between 2 and 6 Gy, the hematopoietic (HP) injury is expected to be the major contribution to the mortality of victims that occurs within weeks after exposure. In this case, acute radiation exposure triggers the death of hematopoietic stem cells and progenitor cells leading to

myelosuppression and increased susceptibility to infection, hemorrhage and anemia. After exposure to higher doses between 6 and 10 Gy, victims develop both irreversible HP and gastrointestinal (GI) injuries. Radiation-induced GI syndrome is characterized by death of GI stem/progenitor cells, drastic functional dysregulation of the intestinal epithelium and loss of digestive barrier integrity. Victims suffer from abdominal pain, diarrhea, dehydration, intestinal bleeding and sepsis, and mortality occurs within 2 weeks after exposure. Because the time window of opportunity for intervention is very short, between 24 and 48 hours after exposure, most drugs under investigation are radioprotectors or radiomitigators. Nevertheless, in 2006, a European consensus was established for the treatment of accidental radiation-induced HP syndrome [1, 2]. This treatment involves acute administration of a cytokine combination to stimulate residual hematopoiesis. In the case of irreversible medullar aplasia, bone marrow transplantation could be used. Although these treatments were efficacious for HP syndrome management, they were not able to rescue GI syndrome in experimental models [3, 4] Consequently, GI syndrome remains intractable to clinical intervention and is lethal for patients exposed to high doses of radiation.

An innovative therapy using the administration of mesenchymal stromal cells (MSC) has been proposed for treatment of GI alterations in a context of ARS syndromes [5, 6]. MSC have been reported to have pleiotropic properties, and have been tested in more than 1000 clinical trials for the treatment of a wide range of diseases (http://www.clinicaltrials.gov), including of the bone marrow and GI tract. In 2006, it was proposed that MSC exert their therapeutic effects through secretion of bioactive factors [7, 8]. An emerging consensus highlights that most of the paracrine physiological functions of MSC are related to their potential to release extracellular vehicles (EVs), namely MSC-derived small EVs/exosomes and/or microvesicles [9, 10]. Similarly, the therapeutic benefits of MSC for radiation-induced intestinal toxicity might also be attributed to the release of MSC-derived exosomes which were already implicated as the mediator of MSC protection in necrotizing enterocolitis of the intestine [11].

Exosomes are bilipid membrane nanovesicles (30–100 nm) produced by intracellular endosomes and released into the extracellular environment after fusion with the plasma membrane. Exosomes contain proteins such as growth factors, adhesion molecules, heat shock proteins, cytoplasmic enzymes and signal transduction proteins, but also functional messenger RNA (mRNA) and microRNA. MSC-derived exosomes, like MSC themselves, are very attractive as they might be useful clinical tools for therapeutic cargo delivery to injured cells and as key mediators of signaling within the stem cell niche.

In this context, the aim of this study was to test the effect of MSC-derived small EVs including exosomes on radiation-induced GI toxicity. We used a model of mice subjected to lethal WBI in order to mimic the overlapping of multiorgan failure observed in ARS. To assess the therapeutic benefit of MSC-derived small EVs/exosomes, we chose a WBI dose of 10 Gy, inducing, as we reported, myelosuppression and high transient rupture of the intestinal barrier. We demonstrated that short-term MSC-derived small EV/exosome treatment significantly delayed time to death in the WBI animals and this delay could be attributed to the maintenance of intestinal barrier integrity.

Material And Methods

All experiments were performed in compliance with the Guide for the Care and Use of Laboratory Animals, French regulations for animal experiments (Ministry of Agriculture Order No. B92-032-01, 2006) and European Directives (86/609/CEE) and were approved by the local ethics committee of the institute (permit number: D92-032-01, APAFIS#6503-2016082311257373v2).

Irradiation protocol

Male NUDE mice (Janvier SA, Le Genest St Isle, France) 6/8 weeks of age were received and housed in a temperature-controlled room (21 ± 1 °C). They were allowed free access to water and fed standard pellets. Mice were anesthetized by ketamine and xylazine preparation 2:1 (v/v) mixture diluted in 0.9% NaCl, injected at 0.1 mL/g and a single WBI dose was delivered by a medical accelerator (Alphée). Alphée is an accelerator-type radiation source (maximal energy 4 MeV with an average energy of about 1.5 MeV; 30 kA). The doses used were 15, 13, 12 and 10 Grays (Gy).

Preparation and administration of MSC-derived small EVs/exosomes

All isolations and characterizations were performed as previously described [12, 13], but with some modifications. Briefly, immortalized E1-MYC 16.3 human embryonic stem cell-derived MSCs were cultured in DMEM (GE Healthcare, USA) with 10% fetal bovine serum (FBS) (Thermofisher Scientific, Waltham, MA, USA). To obtain small EVs/exosomes, 80% confluent cells were grown in a chemically defined medium for 3 days and conditioned medium was harvested as previously described (ref: PMID 17565974). The conditioned medium was clarified of cell debris, size fractionated and concentrated 50X by tangential flow filtration using a membrane with a molecular weight cut-off (MWCO) of 100 kDa (Sartorius, Gottingen, Germany). Small extracellular vesicle yield was assayed by protein concentration using a NanoOrange Protein Quantification Kit (Thermofisher Scientific). Each batch of small extracellular vesicle preparation was qualified for particle size distribution (See below: Nanoparticle Tracking Analysis) and presence of exosome-associated markers (See below Transmission Electron Microscopy).

The MSC-derived small EVs/exosomes were lyophilized by Paracrine Therapeutics using a proprietary technique, stored at − 20 °C and re-constituted with water for use. A total of 600 µg of MSC-derived small EVs/exosomes was intravenously administered in three injections of 200 µg, 6 h, 24 h and 48 h after 10 Gy WBI. Controls received vehicle.

Nanoparticle tracking analysis

Exosome was diluted 3000x with 0.22 µm filtered PBS. The size distribution of exosomes was then measured and analyzed by Zetaview® (Particle Metrix GmbH, Meerbusch, Germany) according to the manufacturer's protocol.

Transmission electron microscopy

Glow-discharged EM grids coated with formvar-carbon (EMS) were floated on a 20-µL drop of purified exosome fraction. Excess fluid was blotted away by filter paper and exosomes adhering to the grid surface were immune-labeled with mouse monoclonal anti-CD81 antibody (Santa Cruz Sc-7637) followed by goat anti-mouse secondary antibody coupled with 6 nm gold (EMS). Finally, grids were fixed with 1% glutaraldehyde (EMS), washed and embedded in a thin film of uranyl acetate-methylcellulose (mixture of 4% uranyl acetate and 2% methylcellulose in 1:9 ratio) using the wire loop technique. Samples were analyzed under a JEOL transmission electron microscope (JEM-1010) operated at 80 kV and equipped with an SIA model 12C 4K CCD camera.

Survival curve analysis

NUDE mice were exposed to 15 Gy, 13 Gy, 12 Gy or 10 Gy lethal doses of WBI. The therapeutic effect of MSC-derived small EVs/exosomes was only assessed in NUDE mice subjected to 10 Gy WBI. Animal survival was monitored every 12 h.

Histology methods

Formalin-fixed, paraffin-embedded small intestines were cut at 5 ∝m on a rotary microtome (Leica Microsystems AG, Wetzlar, Germany) and mounted on polysine slides. Sections were deparaffinized in xylene and rehydrated through ethanol baths and PBS. Hydrated sections were stained with hematoxylin, eosin and saffron (HES). The sections were studied for histological changes in the mucosa of the small intestine and morphometric analyses were performed. We evaluated surviving crypts as a percentage of crypt containing 10 or more adjacent chromophilic cells and a lumen, villus height in µm of the small intestine. For each section of the small intestine, 30 to 100 measurements (depending on the severity of the lesion) were performed using image analysis software (Visiolab, Biocom, France).

Immunohistochemistry

Hydrated sections were dipped into permeabilization solution consisting of 0.1% Triton X-100 in PBS and were rinsed in a distilled water bath for 5 min. Then, endogenous enzymes were blocked using 3% hydrogen peroxide (H_2O_2) in methanol for 10 min and washed again in a 50 mM Tris buffer containing 9 g/L NaCl (TBS). To expose masked epitopes, tissues were incubated for 30 min in 10 mmol/L buffered citrate, pH 6.0. Non-specific antibody binding was minimized by incubating sections with protein-block solution (DakoCytomation X0909, DakoCytomation, Courtaboeuf, France) for 30 min. Tissues were incubated in the presence of the primary antibody, Ki67 polyclonal rabbit anti-rat antibody (abcam ab66155) or claudin-3 polyclonal rabbit anti-rat (Thermofisher, PA-16867) at a dilution of 1:1000 and 1:100, respectively, in Dako antibody diluent for 60 min at 37 °C in a humidified chamber. Sections were rinsed in PBS buffer and then incubated with Envision kit anti-mouse HRP (K4002, DakoCytomation) for 30 min at RT. Staining was developed with Histogreen substrate (E109, Eurobio, Les Ulis, France). Sections were counterstained with nuclear fast red (H3403, VectorLabs, Burlingame, CA, USA), dehydrated and mounted. Isotype control antibodies were used as negative controls. Proliferating cells were determined using image analysis software (Visiolab). A minimum of 30 crypts per section were

measured. For each crypt, we evaluated the number of KI67-positive epithelial cells and expressed the results as the percentage of positive cells per crypt.

TUNEL staining

Hydrated sections were incubated in citrate buffer pH 6 for 3 cycles of 5 min in a 600W microwave oven, with 3 in between each followed by 5 min in tap water. Slides were saturated for 30 min with PBS BSA 1%, rinsed in PBS three times and stained with the in-Situ Cell Death Detection Kit (Roche Diagnostics) according to the manufacturer's guidelines. Slides were mounted with DAPI (Vector Laboratories, USA). Apoptotic cells were determined using image analysis software (Visiolab). A minimum of 30 crypts per section were measured. For each crypt, we evaluated the number of TUNEL-positive epithelial cells and expressed the result as the percentage of positive cells per crypt.

In vivo intestinal permeability assay

In vivo intestinal permeability was assessed using fluorescein dextran (FITC-Dextran 4, Sigma-Aldrich) as previously described [14]. Mice were orally gavaged with 0.75 mg/g body weight of 4 kDa FITC-labeled dextran and blood samples were obtained from the retro-orbital venous plexus 5 h after this administration. Blood samples were centrifuged for 10 min at 5000 rpm and plasma was taken and frozen at -20 °C and analyzed the following day. Intestinal permeability to 4 kDa FITC-labeled dextran was determined by measuring the fluorescence intensity in plasma at 485 nm/525 nm using an automatic Infinite M200 microplate reader (Tecan, Lyon, France).

Statistical analysis

Data are given as mean ± S.E.M. (standard error of the mean). Results were compared between groups by one-way ANOVA followed by a Tukey test using GraphPad 7.0 software (GraphPad, San Diego, CA). Results were also compared between groups through normal or Poisson regression models according to the nature of the parameter of interest, continuous response (villus height and intestinal permeability) or count data (apoptosis and proliferation), respectively.

Mouse survival curves were calculated by the Kaplan–Meier method and the P-value was determined by a log-rank test possibly adjusted for multiple comparisons. The Cox survival model was used in the assessment of the association between MSC-derived exosome treatment and risk of death [15]. The coefficients in a Cox regression relate to hazard, which quantifies an increase in the risk or a protective effect according to the sign of the fitted coefficients (positive or negative respectively). Significance analyses were set at ***$p \leq 0.0001$, ** $p \leq 0.001$, *$p \leq 0.05$ vs control, and at $^{§§§}p \leq 0.0001$, $^{§§}p \leq 0.001$, $^{§}p \leq 0.05$ vs the 10 Gy WBI group. The regression and survival analysis were conducted using MATLAB Version: 8.2.0.701 (R2013b) and the graphical representations were generated using GraphPad 7.0 software (GraphPad, San Diego, CA).

Results

Characterization of the NUDE mouse model: WBI-induced severe hematopoieticinjury is associated with dose-dependent small intestine damage.

In this part of the study using a model of severe injury-induced death, we determined the limiting doses of WBI that induce rupture of the gut barrier. Mice were subjected to decreasing lethal WBI doses between 15 and 10 Gy. Reduction in WBI doses was associated with an increase in mouse survival time (figure 1). Maximum mouse survival time was 7 days for 15 Gy, 8 days for 13 or 12 Gy and 9 days for 10 Gy. Moreover, the risk of instantaneous death after 10 Gy was reduced by a factor of 3.75 compared to 15 Gy ($p \leq 0.001$, Cox model) and by 2.75 compared to 13 Gy ($p \leq 0.05$, Cox model). No difference in the risk of instantaneous death was observed between mice subjected to 12 or 10 Gy. Reducing doses also led to less weight loss, 5 days after irradiation (in supplementary data 1, $p \leq 0.001$ for all tested doses *vs* control mice). There was similar weight loss in mice receiving 15 or 13 Gy (in supplementary data 1, 28 and 30% loss *vs* control mice) and in mice receiving 12 or 10 Gy (in supplementary data 1, 20% loss *vs* control mice). However, we observed significant differences in weight loss between 15 or 13 Gy *vs* 12 or 10 Gy (in supplementary data 1, for 15 Gy *vs* 12 and 10 Gy $p \leq 0.001$ and for 13 Gy *vs* 12 and 10 Gy $p \leq 0.05$ and $p \leq 0.001$, respectively). For all WBI doses tested, histological analysis showed similar severe damage in bone marrow that was indicative of myelosuppression. Transplantation of total bone marrow in whole body-irradiated NUDE mice did not prevent death (data not shown). Indeed, at all doses of WBI, death seemed to be triggered mainly by intestinal injury. Therefore, we measured crypt cell viability as the first criterion of intestinal injury. Three days after WBI, we showed a dose-dependent effect on the percentage of surviving crypts in the small intestine. Only 10% of the crypts were viable after the highest dose (15 Gy), suggesting an inability of epithelium to repair and regenerate (figure 2a, $p \leq 0.001$ *vs* control mice). In support of this assumption, we also reported severe structural epithelial alterations, shown in figure 2b and in supplementary data 2a respectively by villus atrophy area (reduction of villus height, $p \leq 0.001$ *vs* control mice and crypt depth tendency *vs* control mice), and in supplementary data 2b by ulceration areas (confirmed by the reduction of crypt/villus density, $p \leq 0.001$ *vs* control mice). This was concomitant with a 2.5-fold increase in intestinal permeability (figure 3, 5.21 +/- 0.68 in control mice *vs* 13.51 +/- 2.9 in 15 Gy irradiated mice, $p < 0.001$ *vs* control mice). Fifteen Gy WBI induced severe and irreversible small intestinal disorders and death at between 4 to 7 days.

At the lowest, 10 Gy dose, WBI did not affect crypt viability (figure 2a). Nevertheless, we observed transient (only at 3 days, data not shown at 5 days) disruption of the intestinal barrier as shown by significant villus atrophy (figure 2b, 223.2 +/- 6.6 µm in control mice *vs* 134.8 +/- 3.86 µm in 10 Gy-irradiated mice, $p < 0.001$ *vs* controls) and a 1.9-fold increase of intestinal permeability (figure 3, 5.22 +/- 0.68 mg/mL 4 kDa FITC-labeled dextran in control mice *vs* 9.68 +/-1.63 mg/mL 4 kDa FITC-labeled dextran in 10 Gy-irradiated mice, $p < 0.05$ *vs* control mice). Ten Gy WBI induced short-term small intestinal disorders that although reversible led to death at between 4 to 9 days.

Significant therapeutic benefit of MSC-derived small EVs/exosomes in irradiated NUDE mice developing hematopoietic and intestinal injury overlap

Based on the dose-effect observations, we opted for a dose of 10 Gy WBI for the rest of the experiments. This dose of irradiation generated ARS with severe small intestinal injury, but preserved sufficient surviving crypts to support therapeutic intervention to repair and regenerate the crypts, and provides a first proof of concept for the therapeutic efficacy of MSC-derived small EVs/exosomes in ARS management.

Based on assays evaluating dose-dependent effects of MSC-derived small EVs/exosomes (in supplementary data 3), we chose to administer a total of 600 µg of MSC-derived small EVs/exosomes in three injections of 200 µg, at 6, 24 and 48 h after WBI.

MSC-derived small EVs/exosomes extend life of irradiated NUDE mice

MSC-derived small EVs/exosomes induced significant therapeutic efficacy as shown by their ability to delay 10 Gy WBI-induced death (figure 4, log-rank test $p<0.0001$). Five days after WBI when 50% of mice had died mostly from intestinal toxicity, 100% of mice treated with MSC-derived small EVs/exosomes were still alive. MSC-derived small EVs/exosomes delayed death at the lethal dose of 50% (LD50) in mice by 3.5 days compared to untreated WBI mice. Consistent with these observations, the risk of instantaneous death induced by 10 Gy WBI was reduced by a statistically significant 85% (Cox model hazard ratio=0.15, $p \leq 0.0001$).

MSC-derived small EVs/exosomes reduce gut barrier dysfunction after WBI in NUDE mice.

Measurement of intestinal permeability and immunostaining of some transmembrane proteins of tight junctions were used as indexes of gut barrier function. We demonstrated that 10 Gy WBI induced a transient 1.8-fold enhancement of gut permeability (figure 5a, $p \leq 0.0001$). Three days post-WBI, MSC-derived small EVs/exosomes prevented radiation-induced increased gut permeability as shown in figure 5a, with no significant difference in plasma fluorescein dextran concentrations between irradiated and small EV/exosome-treated and control mice (figure 5a, 5.68 mg/mL and 4.88 mg/mL, respectively). Claudin-3 plays an important role in the safeguarding of gut barrier function. It is a transmembrane protein of tight junctions localized predominantly at the intercellular junctions of the gut epithelium (figure 5b 1,4). Among a set of other proteins of tight junctions such as ZO-1 and occludin (data not shown), only claudin-3 immunostaining in the small intestine decreased drastically 3 days after 10 Gy WBI (figure 5b 2,5). Reduction of junctional claudin-3 level after WBI could in part explain enhancement of intestinal permeability. Treatment with MSC-derived small EVs/exosomes maintained a significant level of claudin-3 immunostaining despite a reduction in expression compared to the basal level. Importantly, claudin-3 remained localized at the membrane junction, signifying preservation of tight junctions (figure 5b 3,6). In conclusion, MSC-derived small EVs/exosomes were able to limit WBI-induced disruption of the small intestinal barrier.

MSC-derived small EVs/exosomes stimulate the renewal of the small intestine and improve the regenerative process in irradiated NUDE mice

We first analyzed the time-dependent effect (1, 2 and 3 days after WBI) of MSC-derived small EVs/exosomes on the level of both apoptotic and proliferating cells in the small intestinal crypts as an index of the regenerative capacity of the epithelium. Villus height as an index of epithelial thickness and therefore of structural integrity was assessed to demonstrate treatment efficacy in epithelium rescue.

Apoptosis analysis (figure 6a)***:***

The physiological level of apoptotic cells per crypt assessed by TUNEL assay in control mice was very low. The average value quantified was 1.50 ± 0.25% apoptotic cells per crypt. One day after 10 Gy WBI, we observed a significant 9-fold increase in apoptotic cells compared to the basal level ($p \leq 0.0001$). This increase was reduced on days 2 and 3, but remained significant at 6- and 3-fold higher than the basal level, respectively ($p \leq 0.0001$ both). Administration of MSC-derived small EVs/exosomes significantly reduced radiation-induced apoptosis of epithelial crypt cells 1 and 2 days post-exposure (3.7% in irradiated and small EV/exosome-treated mice *vs* 13.2% in irradiated mice, $p \leq 0.0001$, and 2.2% in irradiated and small EV/exosome-treated mice *vs* 8.4% in irradiated mice $p \leq 0.0001$, respectively). At 2 days, MSC-derived small EVs/exosomes provided a prompt return to the basal level of epithelial apoptotic cells (2.2% in irradiated and small EV/exosome-treated mice *vs* 1.5% in control mice, p=0.23).

Crypt cell proliferation analysis (figure 6b)***:***

The estimated basal proliferation (proportion of Ki67-positive cells among the analyzed ones) was 27.9 ± 2.4% in control mice. One day and 2 days after WBI, this basal proliferation fell by approximately a third to 20.5 ± 3.80% ($p \leq 0.001$ *vs* control mice) and 19.0 ± 3.6% ($p \leq 0.0001$ *vs* control mice), respectively. Three days after WBI, proliferating crypt cells returned to the basal level (28.9% in irradiated mice *vs* 27.9% in control mice, p=0.49). These results suggested that 3 days after WBI, healing of the small intestinal through crypt cell proliferation was initiated.

MSC-derived small EVs/exosomes promoted a 1.4-fold increase in proliferating cells compared to the basal level at 1 day (39.3% in irradiated and small EV/exosome-treated mice *vs* 27.9% in control mice, p=0.0004) and 1.2-fold at 2 days with borderline significance (34.4% in irradiated and small EV/exosome-treated mice *vs* 27.9% in control mice, p=0.07). This MSC small EV/exosome-induced proliferation process returned to the basal level 3 days after WBI (25.1% in irradiated and small EV/exosome-treated mice *vs* 27.9% in control mice, p=0.13). Therefore, MSC-derived small EVs/exosomes induce a rapid but transient acceleration in crypt cell proliferation, and possibly promote epithelial renewal.

Structural analysis:

As shown in figure 7, the villus height measured in control mice was 223.2 ± 5.0 µm. Ten Gy WBI at 3 days led to partial epithelial atrophy, corresponding to a significant reduction of villus height to 133.5 ± 5.1 µm ($p \leq 0.0001$ *vs* control mice). Villus height in irradiated mice after administration of MSC-derived small EVs/exosomes was 159.8 ± 9.2 µm, corresponding to a significant 20.0% rise compared to the average value obtained in irradiated mice (p=0.016). This part of the study demonstrated the rapid action

of MSC-derived small EVs/exosomes in preventing loss of structural mass in the small intestine, possibly by increasing cellular proliferation and reducing apoptosis.

Discussion

The manifestation of ARS is multifactorial and involves several overlapping complex mechanisms. Therefore, the development of therapeutics for this syndrome is challenging. Many studies have shown that MSC-derived small EVs have repair and regenerative effects on many injured organs like heart, kidney, liver, skin and also the intestine [16]. Therefore, we hypothesized that MSC small cellular vesicles with their pleiotropic potency would also be highly efficacious in the management of ARS, a complex injury. In accordance with this hypothesis, we provided the first proof of concept that MSC-derived small EVs are a promising therapeutic for mitigation of radiation-induced toxicity.

It has been previously demonstrated that MSC-derived small EVs with their complex cargo of proteins, RNA and lipids have the capacity to participate simultaneously in a wide spectrum of biochemical and cellular activities [17]. The benefit of the MSC-derived small EVs seems to be directly correlated with their ability to improve and alleviate the repair or injurious processes simultaneously as they occur during tissue repair and recovery. This capacity is critical in treating complex injuries and so is advantageous for ARS management. In support of this proposal, MSC-derived small EVs have been reported to have multiple activities, such as immunomodulation [18], anti-apoptosis and pro-survival [19], decrease of oxidative stress [20], promotion of angiogenesis and re-epithelization [9]. Moreover, several recent studies have reported that MSC-derived small EVs exert their therapeutic effects through the concomitant modulation of several processes, such as increased ATP synthesis, activation of survival kinase signaling and decrease of oxidative stress [20]. Furthermore, their effect on osteochondral defects appears through the activation of multiple pathways by enhancing proliferation, decreasing apoptosis and modulating immune activity using different components in their cargo [21].

The terms “MSC-derived small EVs” and “microvesicles” refer to two different EV types. The distinction between them is their biogenesis. MSC-derived small EVs are derived from endosomes [22, 23], while microvesicles are derived from plasma membrane [24, 25]. Isolation of different EV types by their biogenesis is currently not practical or possible because currently we lack specific biomarkers. Size and density of EVs are commonly used for their isolation, but cannot distinguish among the different EV types, whose biophysical parameters overlap. Therefore, all MSC-derived EV preparations described to date are probably heterogeneous mixtures of different EV types of unknown biogenesis. In this study, we established that at least a fraction of the EVs in our preparation is derived from the endosome and so these EVs are MSC-derived small EVs [26]. However, at least two other EV types have been reported [27]. Since the MSC-derived EVs in our preparation are between 50–200 nm (in supplementary data 4), the term “MSC-derived small EVs” in this paper is synonymous with “MSC-derived exosomes” as per recent recommendations [28, 29].

Here, we report that the administration of MSC-derived exosomes increases through several processes the length of survival of mice that developed multiorgan injuries after exposure to 10 Gy WBI. As GI syndrome is the critical limitation in combatting ARS effectively, we chose to focus on assessing the efficacy of MSC exosomes in rescuing radiation-induced GI mucosal barrier integrity. Barrier impairment could lead to life-threatening sepsis. Since sepsis is a major cause of death in GI syndrome [30] and the GI mucosal barrier is highly sensitive to radiation, preservation of this barrier is a major therapeutic target [31]. Here we show that the effectiveness of MSC exosomes against radiation-induced intestinal toxicity is mediated by their ability to maintain intestinal barrier integrity by enhancing mucosal renewal and limiting intestinal permeability.

One of the manifestations of radiation-induced small intestinal toxicity is loss of the self-renewal ability of the epithelium and the subsequent mucosal atrophy associated with dysregulation of the apoptosis/proliferation balance. This can lead to mucosal barrier alteration. In this study, we observed that mucosal atrophy in mice after exposure to 10 Gy WBI was minimized by MSC-derived exosomes. Increase in mucosal thickness is likely mediated by the ability of MSC-derived exosomes to protect epithelial cells from apoptosis and to promote their proliferation. Our results demonstrate that, after 10 Gy WBI, epithelial renewal occurs faster in mice treated with MSC-derived exosomes than in untreated mice. These results are consistent with a previous in vitro observation that irradiation enhances internalization of MSC-derived exosomes in epithelial cells leading to an increase of recipient cell viability [32]. The protection of other epithelial cell types by administration of MSC-derived exosomes has already been described for cutaneous wound healing [33], kidney toxicity rescue [34] and liver regeneration [35].

Another manifestation of radiation-induced GI toxicity is the enhancement of permeability in the GI mucosa after barrier disruption. Ten Gy WBI led to rapid and drastic increase in gut permeability which in our experiments may result from barrier impairment in both small intestinal and colonic mucosa. The colon is a part of the gut that is the primary source of pathogens and toxins, meaning that it is sensitive to stress-induced endotoxemia and bacteremia. Shukla et al showed that the colonic mucosal barrier is highly sensitive to radiation, more than the barrier formed by the small intestinal epithelium [31]. After 10 Gy WBI, although a critical epithelial cell mass is preserved in the small intestine, we observed a partial reduction and disruption of claudin-3, a transmembrane protein of tight junctions, which may reflect barrier dysfunction in this part of the gut in our model. MSC-derived exosomes prevent transient increase of radiation-induced gut mucosal permeability probably by maintaining tight junction functionality, as our results show for claudin-3. MSC-derived exosomes also preserved the gut barrier integrity in a model of necrotizing enterocolitis, an effect associated with their ability to reduce the incidence and severity of the enterocolitis [11]. In part, by reducing/preventing the first steps of radiation-induced intestinal barrier disruption and probably bacterial translocation and inflammatory response, MSC-derived exosomes might provide therapeutic benefits characterized by their ability to delay radiation-induced death. Our results on crypt cell apoptosis/proliferation and epithelial permeability of the irradiated/exosome-treated small intestine show that preservation of gut barrier integrity is one of the decisive parameters that need to be controlled to reduce radiation toxicity. Nevertheless, the therapeutic benefit of MSC-derived exosomes could also be expected to involve partial protection of the HP system. Recent studies have

demonstrated that MSC derived-EVs given after lethal WBI enhance long-term survival. This effect is associated with recovery of HP cells, particularly white blood cells, which probably occurs through MSC-EVs targeting hematopoietic stem cells [36]. Consistent with these studies, we also observed a reduced short-term WBI-induced myelosuppression which was evidenced by hemorrhage reduction and the presence of hematopoietic cells in bone marrow slices from MSC exosome-treated mice (in supplementary data 5). In order to optimize therapy for the management of ARS, the potential effects of MSC-derived exosomes on radiation-induced toxicity in the HP system should be thoroughly investigated and characterized.

The quality of ARS management also depends on the expediency of medical support provided to exposed victims. Schoefinius et al showed that MSC-derived EVs accelerated the kinetics of thrombocyte recovery after lethal WBI compared to MSC themselves [36]. In our study, we also observed that small intestinal mucosa self-renewed more rapidly in mice treated with MSC-derived exosomes compared to mice treated with MSC themselves (data not shown). We noted fast benefits of MSC-derived exosomes, as early as 24 h after WBI, which positions MSC-derived exosomes as a very good candidate for ARS management as they can act quickly on both the HP and GI systems.

So, we provide the proof of concept that MSC-derived exosomes are therapeutically beneficial after WBI. Despite the high doses of MSC-derived exosomes we used in this study, the treatments could only delay but not prevent death in the WBI animals. So far, most of the treatments that provide promising benefits in management of GI syndrome are administered at high frequency and in a long-term iterative process. For instance, BDP/ObreShielf™ (beclomethasone 17,21-dipropionate) provided benefit in radiation-induced GI toxicity when the animals received 2 mg orally every 6 hours for 14 days, then 2 mg orally twice daily until 100 days. Hence, the size and frequency of dosing of MSC exosomes could be important in improving survival of WBI animals. New investigations to test increased therapeutic doses and/or duration of MSC-derived small EV/exosome treatment are currently ongoing.

Moreover, further experiments are needed to fully characterize the mechanisms of action by which MSC-derived exosomes act on the small intestine, but also to establish whether MSC-derived exosomes have an effect on other organs or tissues altered by irradiation.

Conclusions

In summary, our results highlight new therapeutic options for patients suffering from ARS. The mechanism of action we propose for the efficacy of MSC-derived exosomes in delaying radiation-induced death is consistent with the current consensus that preservation of gut barrier integrity is key to the management of radiation toxicity. The administration of MSC-derived exosomes in relation to the use of MSC themselves may have many advantages. Treatment with MSC-derived exosomes is a cell-free therapy and therefore might overcome side effects that could be associated with native MSC treatment, like immune reactions, pulmonary occlusion after systemic administration, ectopic tissue genesis or long-term mal-differentiation of transplanted cells. Moreover, the establishment of exosome banks and the

possibility of lyophilizing MSC-derived exosomes might be valuable in ARS management, especially in the case of large-scale nuclear/radiological events.

Declarations

Authors' contributions

AA: Acquisition of data, analysis and interpretation of data, drafting of the manuscript, BL: Acquisition of data, analysis and interpretation of data, MoBe: Statistical analysis of data, SKL: Provision of material support and editing of the manuscript, CG: Editing of the manuscript, MaBe: Editing of the manuscript, RT: Acquisition of funding, substantial contributions to conception and design, AS: Conception and design, acquisition of data, analysis and interpretation of data, drafting of the manuscript, final approval of the version to be published

Funding: This work was supported in part by The National Institutes of Health (NIH)/NIAID Subcontract n° 5 U19 Al091175 05.

Competing financial interest declaration

The authors declare no conflict of interest.

Availability of data and materials

The datasets generated/analyzed during the current study are available.

Ethics approval and consent

All experiments were performed in compliance with the Guide for the Care and Use of Laboratory Animals, French regulations for animal experiments (Ministry of Agriculture Order No. B92-032-01, 2006) and European Directives (86/609/CEE) and were approved by the local ethics committee of the institute (permit number: D92-032-01, APAFIS#6503-2016082311257373v2)

Consent for publication

Not applicable

Author details

[1]Laboratory of Medical Radiobiology, [2]Department of research in Radiobiology and regenerative medicine, Institute for Radiological Protection and Nuclear Safety, Fontenay-aux-Roses, France.[3]Laboratory of accidental Radiobiology, Department of research in Radiobiology and regenerative medicine, Institute for Radiological Protection and Nuclear Safety, Fontenay-aux-Roses, France. [4]Exosome and Secreted Nano-vesicle Group, ASTAR Institute of Medical Biology , Singapore ; Department of Surgery, Yong Loo Lin School of Medicine, National University of Singapore , Singapore. [5]Department of Radiation

Oncology, Albert Einstein College of Medicine/Albert Einstein Cancer Center, NY, USA. [5]Department of Radiation Oncology, Albert Einstein College of Medicine/Albert Einstein Cancer Center, NY, USA.

Abbreviations

Acute radiation syndrome: ARS, Extracellular vehicles (EVs), Gastrointestinal: GI, Grays (Gy), Hematopoietic: HP, Mesenchymal stromal cells: MSC, Whole-body irradiation: WBI

References

1. Gorin NC, Fliedner TM, Gourmelon P, Ganser A, Meineke V, Sirohi B, et al. Consensus conference on European preparedness for haematological and other medical management of mass radiation accidents. Ann Hematol. 2006;85(10):671-9.
2. Fliedner TM, Chao NJ, Bader JL, Boettger A, Case C, Jr., Chute J, et al. Stem cells, multiorgan failure in radiation emergency medical preparedness: a U.S./European Consultation Workshop. Stem Cells. 2009;27(5):1205-11.
3. Mason KA, Withers HR, McBride WH, Davis CA, Smathers JB. Comparison of the gastrointestinal syndrome after total-body or total-abdominal irradiation. Radiat Res. 1989;117(3):480-8.
4. Terry NH, Travis EL. The influence of bone marrow depletion on intestinal radiation damage. Int J Radiat Oncol Biol Phys. 1989;17(3):569-73.
5. Eaton EB, Jr., Varney TR. Mesenchymal stem cell therapy for acute radiation syndrome: innovative medical approaches in military medicine. Mil Med Res. 2015;2:2.
6. Fukumoto R. Mesenchymal stem cell therapy for acute radiation syndrome. Mil Med Res. 2016;3:17.
7. Caplan AI, Dennis JE. Mesenchymal stem cells as trophic mediators. J Cell Biochem. 2006;98(5):1076-84.
8. Semont A, Demarquay C, Bessout R, Durand C, Benderitter M, Mathieu N. Mesenchymal stem cell therapy stimulates endogenous host progenitor cells to improve colonic epithelial regeneration. PLoS One. 2013;8(7):e70170.
9. Lai RC, Arslan F, Lee MM, Sze NS, Choo A, Chen TS, et al. Exosome secreted by MSC reduces myocardial ischemia/reperfusion injury. Stem Cell Res. 2010;4(3):214-22.
10. Biancone L, Bruno S, Deregibus MC, Tetta C, Camussi G. Therapeutic potential of mesenchymal stem cell-derived microvesicles. Nephrol Dial Transplant. 2012;27(8):3037-42.
11. Rager TM, Olson JK, Zhou Y, Wang Y, Besner GE. Exosomes secreted from bone marrow-derived mesenchymal stem cells protect the intestines from experimental necrotizing enterocolitis. J Pediatr Surg. 2016;51(6):942-7.
12. Chen TS, Arslan F, Yin Y, Tan SS, Lai RC, Choo AB, et al. Enabling a robust scalable manufacturing process for therapeutic exosomes through oncogenic immortalization of human ESC-derived MSCs. J Transl Med. 2011;9:47.

13. Sze SK, de Kleijn DP, Lai RC, Khia Way Tan E, Zhao H, Yeo KS, et al. Elucidating the secretion proteome of human embryonic stem cell-derived mesenchymal stem cells. Mol Cell Proteomics. 2007;6(10):1680-9.
14. Tambuwala MM, Cummins EP, Lenihan CR, Kiss J, Stauch M, Scholz CC, et al. Loss of prolyl hydroxylase-1 protects against colitis through reduced epithelial cell apoptosis and increased barrier function. Gastroenterology. 2010;139(6):2093-101.
15. Cox C. Multinomial regression models based on continuation ratios. Stat Med. 1988;7(3):435-41.
16. Phinney DG, Pittenger MF. Concise Review: MSC-Derived Exosomes for Cell-Free Therapy. Stem Cells. 2017;35(4):851-8.
17. Lai RC, Chen TS, Lim SK. Mesenchymal stem cell exosome: a novel stem cell-based therapy for cardiovascular disease. Regen Med. 2011;6(4):481-92.
18. Zhang B, Yin Y, Lai RC, Tan SS, Choo AB, Lim SK. Mesenchymal stem cells secrete immunologically active exosomes. Stem Cells Dev. 2014;23(11):1233-44.
19. Lai RC, Yeo RW, Tan KH, Lim SK. Mesenchymal stem cell exosome ameliorates reperfusion injury through proteomic complementation. Regen Med. 2013;8(2):197-209.
20. Arslan F, Lai RC, Smeets MB, Akeroyd L, Choo A, Aguor EN, et al. Mesenchymal stem cell-derived exosomes increase ATP levels, decrease oxidative stress and activate PI3K/Akt pathway to enhance myocardial viability and prevent adverse remodeling after myocardial ischemia/reperfusion injury. Stem Cell Res. 2013;10(3):301-12.
21. Zhang S, Chuah SJ, Lai RC, Hui JHP, Lim SK, Toh WS. MSC exosomes mediate cartilage repair by enhancing proliferation, attenuating apoptosis and modulating immune reactivity. Biomaterials. 2018;156:16-27.
22. Harding C, Heuser J, Stahl P. Receptor-mediated endocytosis of transferrin and recycling of the transferrin receptor in rat reticulocytes. J Cell Biol. 1983;97(2):329-39.
23. Pan BT, Johnstone RM. Fate of the transferrin receptor during maturation of sheep reticulocytes in vitro: selective externalization of the receptor. Cell. 1983;33(3):967-78.
24. Cocucci E, Meldolesi J. Ectosomes and exosomes: shedding the confusion between extracellular vesicles. Trends Cell Biol. 2015;25(6):364-72.
25. Raposo G, Stoorvogel W. Extracellular vesicles: exosomes, microvesicles, and friends. J Cell Biol. 2013;200(4):373-83.
26. Tan SS, Yin Y, Lee T, Lai RC, Yeo RW, Zhang B, et al. Therapeutic MSC exosomes are derived from lipid raft microdomains in the plasma membrane. J Extracell Vesicles. 2013;2.
27. Lai RC, Tan SS, Yeo RW, Choo AB, Reiner AT, Su Y, et al. MSC secretes at least 3 EV types each with a unique permutation of membrane lipid, protein and RNA. J Extracell Vesicles. 2016;5:29828.
28. Thery C, Witwer KW, Aikawa E, Alcaraz MJ, Anderson JD, Andriantsitohaina R, et al. Minimal information for studies of extracellular vesicles 2018 (MISEV2018): a position statement of the

International Society for Extracellular Vesicles and update of the MISEV2014 guidelines. J Extracell Vesicles. 2018;7(1):1535750.

29. Witwer KW, Van Balkom BWM, Bruno S. Choo A, Dominici M, Gimona M, et al. Defining mesenchymal stromal cell (MSC)-derived small extracellular vesicles for therapeutic applications. J Extracell Vesicles. 2019 ; 8(1):1609206.
30. Macia IGM, Lucas Calduch A, Lopez EC. Radiobiology of the acute radiation syndrome. Rep Pract Oncol Radiother. 2011;16(4):123-30.
31. Shukla PK, Gangwar R, Manda B, Meena AS, Yadav N, Szabo E, et al. Rapid disruption of intestinal epithelial tight junction and barrier dysfunction by ionizing radiation in mouse colon in vivo: protection by N-acetyl-l-cysteine. Am J Physiol Gastrointest Liver Physiol. 2016;310(9):G705-15.
32. Hazawa M, Tomiyama K, Saotome-Nakamura A, Obara C, Yasuda T, Gotoh T, et al. Radiation increases the cellular uptake of exosomes through CD29/CD81 complex formation. Biochem Biophys Res Commun. 2014;446(4):1165-71.
33. Zhang J, Guan J, Niu X, Hu G, Guo S, Li Q, et al. Exosomes released from human induced pluripotent stem cells-derived MSCs facilitate cutaneous wound healing by promoting collagen synthesis and angiogenesis. Journal of translational medicine. 2015;13:49.
34. Zhou Y, Xu H, Xu W, Wang B, Wu H, Tao Y, et al. Exosomes released by human umbilical cord mesenchymal stem cells protect against cisplatin-induced renal oxidative stress and apoptosis in vivo and in vitro. Stem Cell Res Ther. 2013;4(2):34.
35. Tan CY, Lai RC, Wong W, Dan YY, Lim S-K, Ho HK. Mesenchymal stem cell-derived exosomes promote hepatic regeneration in drug-induced liver injury models. Stem Cell Res Ther. 2014;5(3):76.
36. Schoefinius JS, Brunswig-Spickenheier B, Speiseder T, Krebs S, Just U, Lange C. Mesenchymal Stromal Cell-Derived Extracellular Vesicles Provide Long-Term Survival After Total Body Irradiation Without Additional Hematopoietic Stem Cell Support. Stem Cells. 2017;35(12):2379-89.

Figures

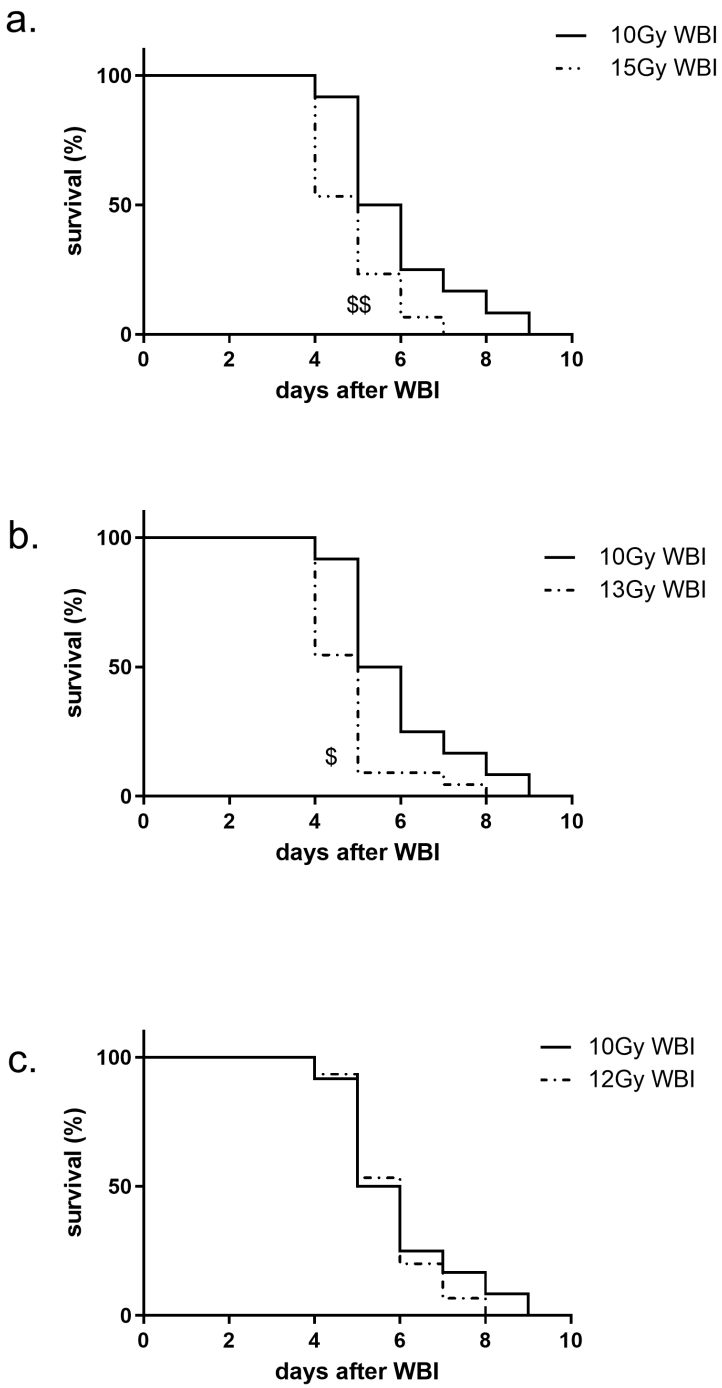

Figure 1

Figure 1

Effect of decreasing lethal doses of WBI on mouse survival. NUDE mice were subjected to 15 Gy, 13 Gy, 12 Gy and 10 Gy lethal doses of WBI. Time points of interventions are given above survival plots. Each value represents cumulative data of 3 independent experiments, (N=3, 23 mice in 10 Gy WBI group, 15 mice in 12 Gy WBI group, 21 mice in 13 Gy WBI and 31 mice in 15 Gy WBI group). Mouse survival curves

were calculated by the Kaplan–Meier method and the P-value was determined by the log-rank test and the Cox model, $p≤0.05 $$p≤0.001 compared to the 10 Gy WBI group.

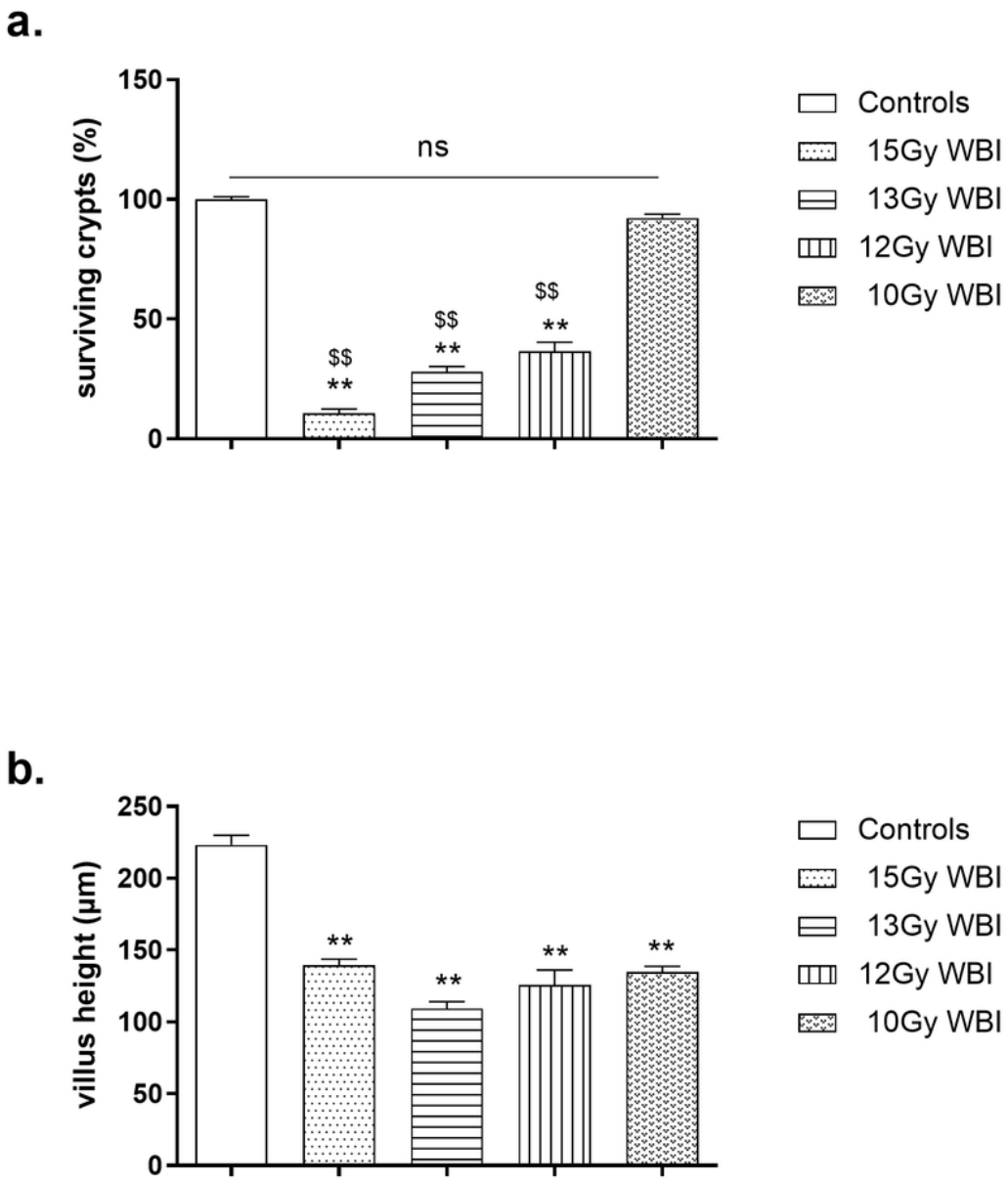

Figure 2

Figure 2

Severity of histological alterations of the small intestine is WBI dose-dependent NUDE mice were subjected to 15 Gy, 13 Gy, 12 Gy and 10 Gy lethal doses of WBI. Three days after WBI, small intestinal sections were stained with hematoxylin-eosin-saffron (HES). Morphometric analysis was performed:

quantitative assessment of (a) the small intestinal crypt viability (in % of surviving crypts containing 10 or more adjacent chromophilic cells and a lumen), and (b) villus height (in µm). Each value represents the average of 30-100 independent measurements (with decreasing doses we observed on each section increased numbers of measurable crypts and villi) from 3 independently repeated experiments (N=3, 4 to 6 animals per group and per experiment). **p≤0.001 compared to the control group, $$ p≤0.001 compared to the 10 Gy WBI group.

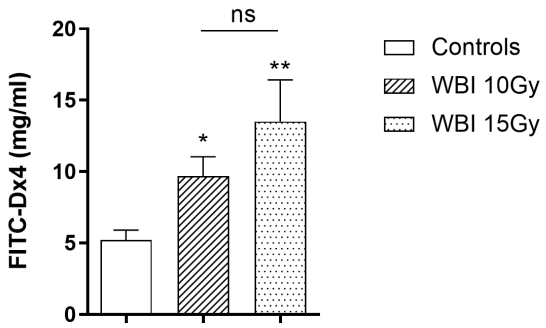

Figure 3

Figure 3

15 Gy and 10 Gy WBI increased gut permeability in NUDE mice at 3 days. Nude mice received 10 Gy or 15 Gy lethal doses of WBI. At 3 days, control and irradiated mice were orally gavaged with 75 mg/mL of 4 kDa FITC-labeled dextran and 5 hours later blood samples were collected. Small intestinal permeability was determined by plasma assay of 4 kDa FITC-labeled dextran (mg/mL). Each value represents the average value from 2 independently repeated experiments, (N=2, 5 to 10 animals per group and per experiment), *p≤0.05, **p≤0.001 compared to the control group.

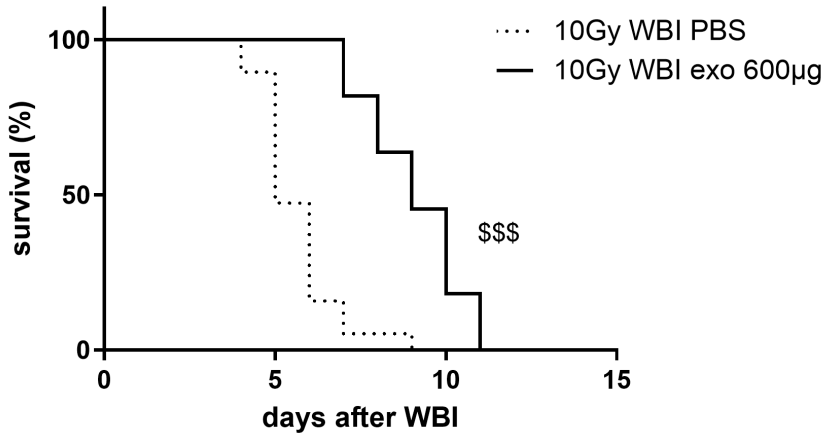

Figure 4

Figure 4

MSC-derived small EVs/exosomes extend the life of NUDE mice subjected to 10 Gy WBI. NUDE mice were subjected to a 10 Gy lethal dose of WBI. A total of 600 μg of MSC-derived small EVs/exosomes was intravenously administered in three injections of 200 μg, 6 h, 24 h and 48 h after WBI. Controls received vehicle. Time points of interventions are given above survival plots. Each value results from one representative experiment, (N=1, 19 mice in 10 Gy WBI group treated with PBS and 11 mice in the 10 Gy WBI group treated with MSC-derived small EVs/exosomes). Mouse survival curves were calculated by the Kaplan–Meier method and the P-value was determined by the log-rank test, where necessary adjusted for multiple comparisons. $$$p≤0.0001 compared to the 10 Gy WBI group. The survival Cox model was used in the assessment of the association between MSC-derived exosome treatment and instantaneous risk of death.

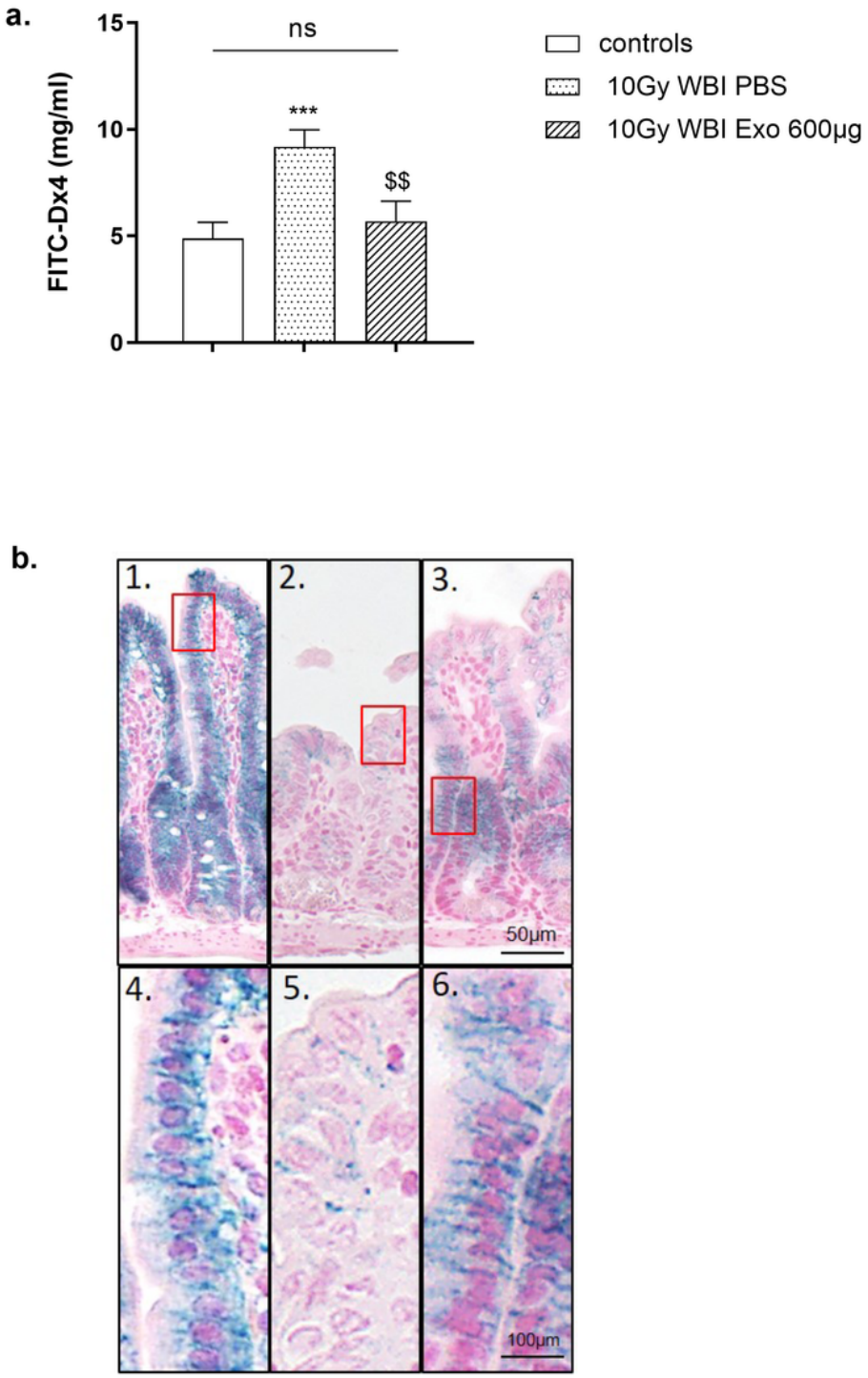

Figure 5

Figure 5

MSC-derived small EVs/exosomes reduce 10 Gy WBI-induced gut permeability at 3 days. Nude mice received 10 Gy WBI. A total of 600 µg of MSC-derived exosomes was intravenously administered in three injections of 200 µg, 6 h, 24 h and 48 h after WBI. Controls received vehicle. (a) At 3 days post-WBI, all mice were orally gavaged with 75 mg/mL of 4 kDa FITC-labeled dextran and 5 hours later blood samples were collected. Small intestinal permeability was determined by plasma assay of 4 kDa FITC-labeled

dextran (mg/mL). Each value represents the average from 3 independently repeated experiments (N=3, 2 to 12 animals per group and per experiment), ***p≤0.0001 compared to the control group, $$p≤0.001 compared to the 10 Gy WBI group. (b) Representative pictures of claudin-3 immunostaining in the small intestine of NUDE mouse controls (1 and 4), 3 days after 10 Gy WBI and treatment with PBS (2 and 5) and 3 days after 10 Gy WBI and treatment with MSC-derived small EVs/exosomes (3 and 6). Scale bar 100 µm for 1, 2 and 3 and 50 µm for 4, 5 and 6.

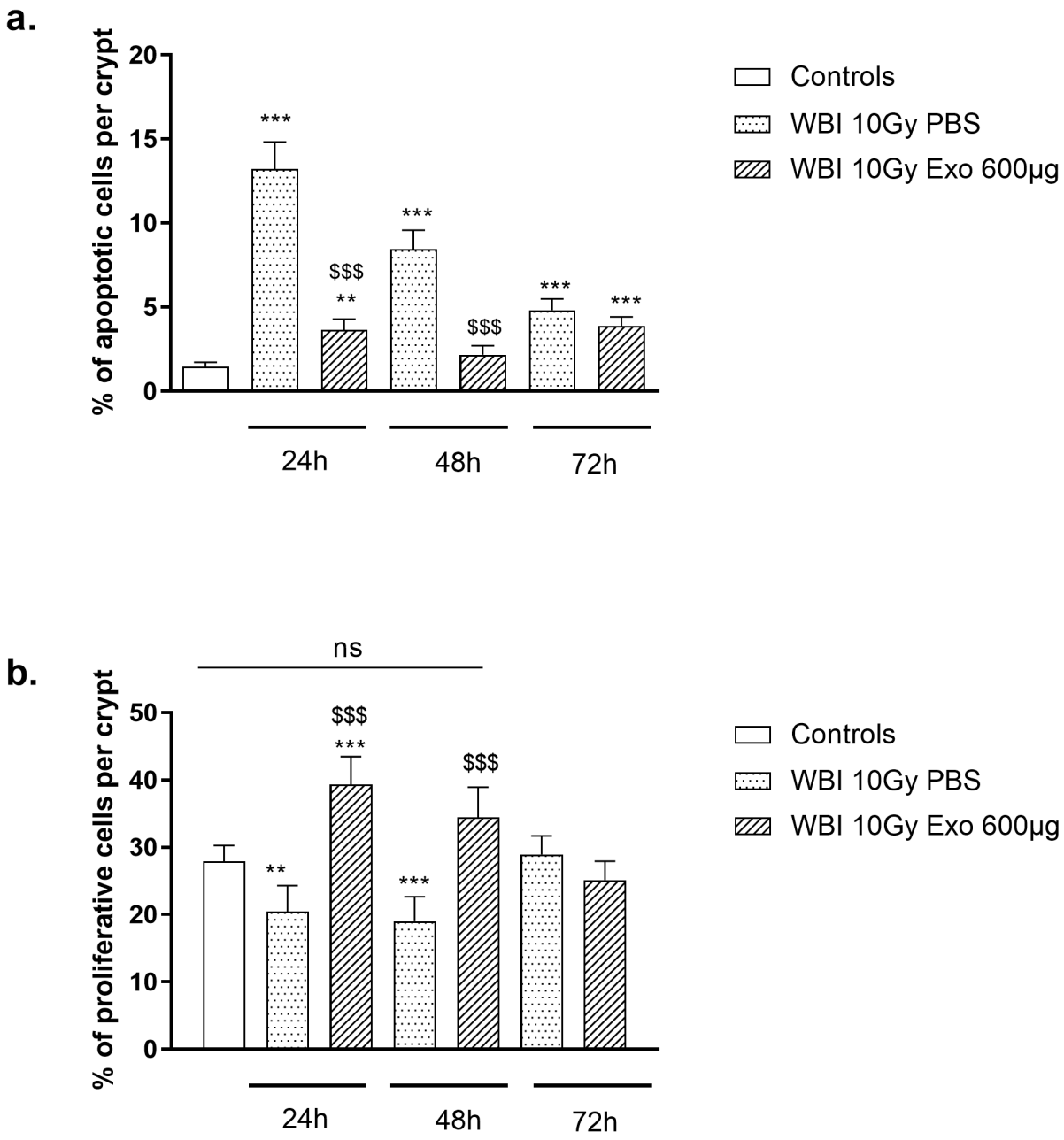

Figure 6

Figure 6

MSC-derived derived small EVs/exosomes reduce 10 Gy WBI-induced epithelial apoptosis and promote their proliferation Nude mice received a 10 Gy lethal dose of WBI. A total of 200 µg (i), 400 µg (ii) or 600 µg(iii) of MSC-derived small EVs/exosomes was intravenously administered respectively in one, two or three injections of 200 µg, 6 h after WBI for (i), 6 h and 24 h after WBI for (ii) and 6 h, 24 h and 48 h after WBI for (iii). Mice were sacrificed 24 h, 48 h or 72 h after WBI. (a) Crypt cell apoptosis was assessed by TUNEL assay and (b) crypt cell proliferation by KI67 immunostaining, in control NUDE mice (respectively 12 and 24 animals), 24 h, 48 h or 72 h after 10 Gy WBI with PBS treatment (respectively 5 and 4 mice at 24 h, 6 and 5 mice at 48 h, and 6 and 17 mice at 72 h) or MSC-derived small EV/exosome treatment (respectively 7 and 6 mice at 24 h, 6 and 5 mice at 48 h, and 6 and 7 mice at 72 h). Each value represents the average of 30 independent crypt measurements per slice and is expressed as a percentage of the control value, N=1. **p≤0.001, ***p≤0.0001 compared to the control group; $$$p≤0.0001, for each time the 10 Gy WBI group treated with small EVs/exosomes was compared to the 10 Gy WBI group treated with PBS.

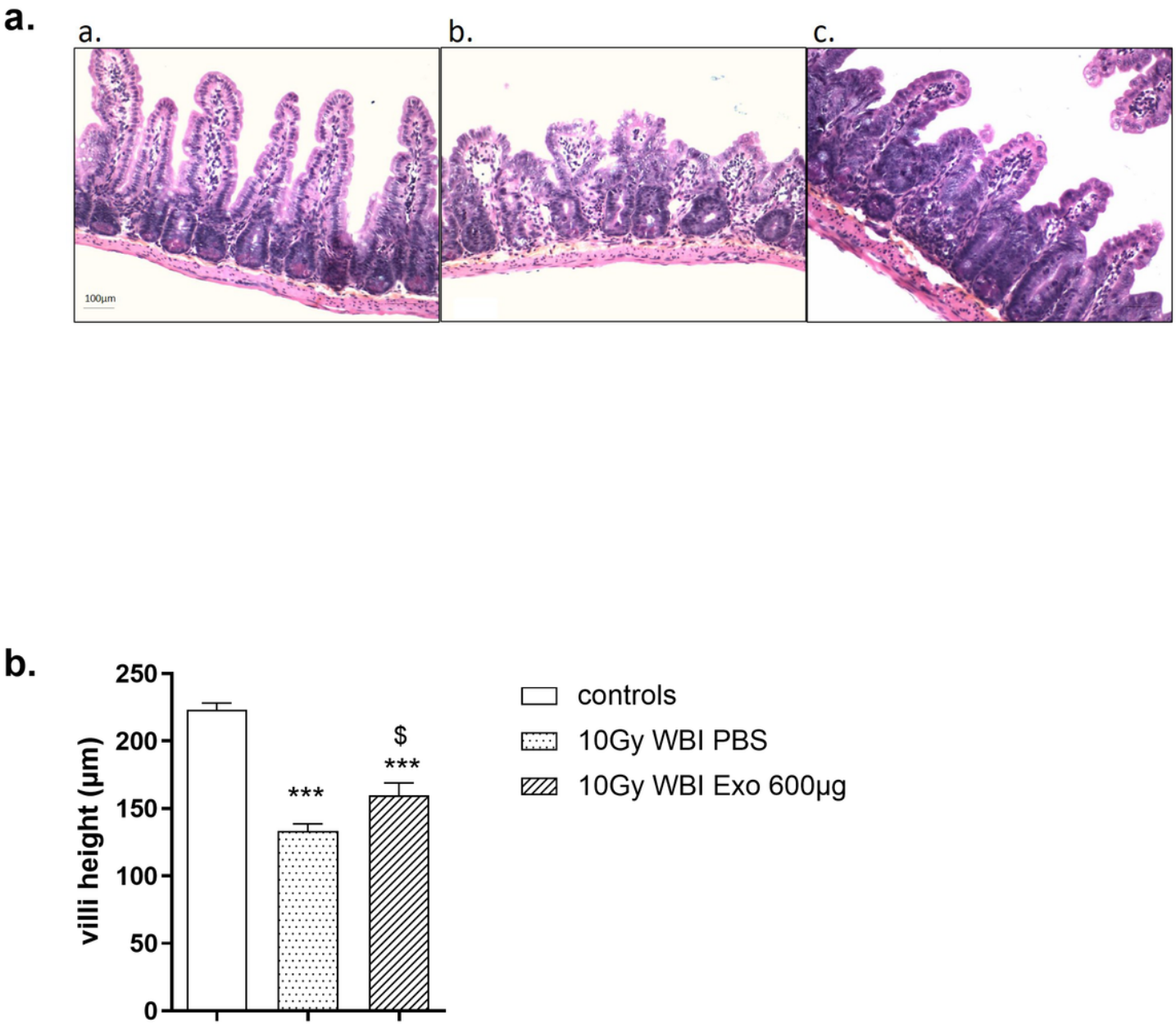

Figure 7

Figure 7

MSC-derived small EVs/exosomes minimize 10 Gy WBI-induced alteration of small intestinal structure at 3 days Nude mice received a 10 Gy lethal dose of WBI and were sacrificed at 3 days. A total of 600 µg of MSC-derived small EVs/exosomes was intravenously administered in three injections of 200 µg, 6 h, 24 h and 48 h after WBI. Controls received vehicle. (a) Small intestinal sections were stained with hematoxylin-eosin-saffron (HES). Representative pictures of small intestinal slices from control mice (aa), mice subjected to 10 Gy WBI and treated with PBS (ab) and mice subjected to 10 Gy WBI and treated with

MSC-derived small EVs/exosomes (ac). Scale bar 100 μm. (b) Quantitative analysis of villus height of the small intestine (μm). Each value represents the average of 20-30 independent measurements per animal from 3 independently repeated experiments (N=3, 6 to 8 animals per group and per experiment). ***p<0.0001 compared to the control group, $ p<0.05 compared to the 10 Gy group.

Supplementary Files

This is a list of supplementary files associated with this preprint. Click to download.

- supplementarydata5.tif
- Supplementarydata2.tif
- Supplementarydata1.tif
- supplementarydata4.tif
- Supplementarydata3.tif